PROCEEDINGS OF SCIENCE

Do two-dimensional correlation data falsify RHIC paradigms?

Lanny Ray* **for the STAR Collaboration**
Department of Physics, The University of Texas at Austin, Austin, Texas 78712 USA
E-mail: ray@physics.utexas.edu

Two-particle, two-dimensional charged particle correlations on transverse momentum and on relative pseudorapidity and azimuth, obtained for p-p, Au-Au and Cu-Cu minimum-bias collisions from the STAR experiment at RHIC enable unique studies of the dense, strong-force systems formed in these collisions as these systems evolve with increasing collision energy and number of colliding nucleons. Most of the correlation structures observed in p-p and peripheral A-A collisions are readily interpreted in terms of perturbative QCD and established fragmentation phenomenology. Significant changes occur in the correlation structures with increasing centrality. The centrality evolution is presently not understood and these data challenge theoretical models, perhaps falsifying some of those presently available. A summary of the present experimental information and a discussion of the constraints which the body of two-particle, 2D correlation data impose on RHIC paradigms and proposed theoretical models are presented.

Workshop on Critical Examination of RHIC Paradigms - CERP2010
April 14-17, 2010
Austin, Texas USA

*Speaker.

PoS(CERP2010)015

1. Introduction

A major goal of the RHIC program is to learn something new about QCD by studying novel, strong-force systems such as the dense environment produced in relativistic heavy-ion collisions. However, determining the type of data which will unambiguously reveal new manifestations of QCD and which will test, and perhaps falsify, the proposed paradigms for relativistic heavy ion collision dynamics is non-trivial. In this presentation I will review results of two-particle correlation data and analyses from the STAR experiment and will show that these data uniquely challenge RHIC paradigm interpretations and may ultimately provide the experimental basis for new insights into how QCD works in highly dense large-volume systems. The focus here is on two specific correlation structures: (1) the same-side (relative azimuth $< \pi/2$), pseudorapidity (η) elongated peak at zero relative opening angle [1,2] and (2) the corresponding away-side ($> \pi/2$) ridge. The evolution of both structures is studied with respect to collision energy, centrality and transverse momentum.

The philosophy behind the present analysis is simple. We begin with proton-proton (p-p) collisions and try to understand those data in terms of perturbative QCD (pQCD), parton distribution functions (PDF), and fragmentation functions (FF); then we move on to nucleus-nucleus (A-A) collisions of increasing centrality, comparing the results to the p-p reference data. In the viewpoint advocated here the logical starting point in attempting to understand A-A data is in terms of pQCD, PDFs and FFs where modifications may occur in each component. Shadowing and gluon saturation affect the PDFs. Novel QCD diagrams may become important in the dense heavy-ion collision environment. Fragmentation functions may be modified in A-A compared to that in p-p or e^+-e^-. Rescattering among the partonic or hadronic constituents may occur, but may or may not have significant effects on the final state observables. Our philosophy is that only when these pQCD-based mechanisms have been accounted for is one permitted to invoke more complex dynamical processes to explain the data, e.g. equilibration, hydrodynamics. New physics may be invoked to explain the A-A data only when the data require it.

2. Two-particle correlation analysis

The correlation data presented here were obtained using the reconstructed, charged particle trajectories (tracks) in the STAR Time Projection Chamber (TPC) [3] with transverse momentum $p_t > 0.15$ GeV/c, $|\eta| < 1$ and 2π azimuth. The six-dimensional momentum space correlations were projected onto 2D transverse momentum, (η_1,η_2), (ϕ_1,ϕ_2) and (η_Δ,ϕ_Δ) subspaces, where $\eta_\Delta = \eta_1 - \eta_2$ and $\phi_\Delta = \phi_1 - \phi_2$. For symmetric collision systems (e.g. Au-Au but not d-Au) the (η_1,η_2) and (ϕ_1,ϕ_2) correlations are approximately invariant with respect to $\eta_1 + \eta_2$ and $\phi_1 + \phi_2$, over the STAR TPC acceptance [4]. We may therefore consider only the 2D angular correlation subspace (η_Δ,ϕ_Δ) without loss of information. For the 2D transverse momentum correlations improved visual access to both the lower and higher p_t correlation structures is afforded by plotting the data on a $\sim \log(p_t)$ variable, specifically transverse rapidity, $y_t = \log[(p_t + m_t)/m_\pi]$, where m_t is transverse mass and m_π is the pion mass. Choice of pion mass to regulate the behavior of y_t in the limit $p_t = 0$ is arbitrary for the present non-identified particle analysis. For visual clarity what matters is that this mass be smaller than the characteristic p_t/c of the correlation structures of interest. Selection

of the mass parameter similar to the minimum p_t acceptance (150 MeV/c) leaves the simple $\log(p_t)$ dependence intact over most of the momentum range relevant here.

Two-dimensional transverse rapidity correlations on (y_{t1},y_{t2}) provide independent information from that in the angular correlations, for example identification of correlation structures which may originate from "soft" or "hard" QCD processes. 2D (η_Δ,ϕ_Δ) correlations obtained from pair cuts in selected regions of (y_{t1},y_{t2}) subspace and vice-versa enable further access to the 6D correlation information and provide additional clues to the origins of these structures.

The 2D (y_{t1},y_{t2}) and (η_Δ,ϕ_Δ) correlations were obtained via unit integral normalized ratios of real to mixed-event pairs within each 2D bin in the subspace. The specific correlation measure used here is defined as [2],

$$\Delta\rho/\sqrt{\rho_{ref}} = \sqrt{\rho'_{ref}}(\Delta\rho/\rho_{ref}) = \sqrt{\rho'_{ref}}\,[(\rho_{sib}-\rho_{ref})/\rho_{ref}] \ , \tag{2.1}$$

where ρ_{sib} and ρ_{ref} represent real and mixed-event binned pair densities, respectively. Bin-wise ratio ρ_{sib}/ρ_{ref} cancels detector acceptance and single particle reconstruction efficiency effects. STAR track quality selection criteria are discussed in [1,2]. Two-track reconstruction inefficiencies for charged-particle trajectories occurring at small separation distances (< few cm) in the TPC tracking volume required additional corrections [1,4]. Prefactor $\sqrt{\rho'_{ref}}$ was obtained as the geometric mean of the product of corrected single particle densities $[\mathrm{d}^3\mathrm{N}_{ch}/\mathrm{d}y_{t1}\mathrm{d}\eta_1\mathrm{d}\phi_1] \times [\mathrm{d}^3\mathrm{N}_{ch}/\mathrm{d}y_{t2}\mathrm{d}\eta_2\mathrm{d}\phi_2]$ projected onto the appropriate subspace. Quantity $\Delta\rho/\sqrt{\rho_{ref}}$ corresponds to Pearson's normalized covariance from statistics. It can be interpreted as a bin-wise number of correlated pairs per final state particle and is designed to test the null hypothesis that A-A collisions are equivalent to a Glauber linear superposition (GLS) of independent nucleon-nucleon minimum-bias collisions.

3. Correlations from minimum-bias p-p collisions

Transverse rapidity and angular correlations for 200 GeV minimum-bias p-p collisions [5] are shown in the upper two panels of Fig. 1. The lower row of figures presents angular correlations for charged particle pairs selected with respect to $y_{t\Sigma} = y_{t1} + y_{t2}$ either less than 4 (left panel) or greater than 4 (right panel) corresponding to the lower and higher y_t correlation structures in the upper-left panel. The $y_{t\Sigma}$ cut corresponds to single particle p_t of order 0.5 GeV/c. The angular correlations are quite different. The lower y_t projection displays an azimuth independent ridge on η_Δ plus a narrow peak at (0,0) while the higher y_t pair distribution manifests a much larger peak at (0,0) and an η_Δ independent ridge on ϕ_Δ, centered at $\phi_\Delta = \pi$. Comparison of like-sign (LS) and unlike-sign (US) charged pair correlations suggests that the lower y_t angular structures are due to charge-ordering [6] from longitudinal fragmentation (i.e. the ridge on η_Δ in the lower-left panel), plus a combination of quantum correlations and e^+-e^- pair production backgound for the sharp peak at (0,0). The larger y_t angular correlations display a classic back-to-back di-jet structure corresponding to pairs of correlated particles with $p_t \sim 1$ - 1.5 GeV/c ($y_t \sim 3$).

Experiment UA1 [7] reported jet-like energy clusters down to about 5 GeV (detector background limited) in $\sqrt{s}$ = 200 GeV proton-antiproton collisions, and the resulting transverse energy distributions agreed with pQCD calculations. In the STAR p-p (y_{t1},y_{t2}) correlation data we observe a peak structure consisting of at least two correlated particles, each having p_t of order 1 to 1.5

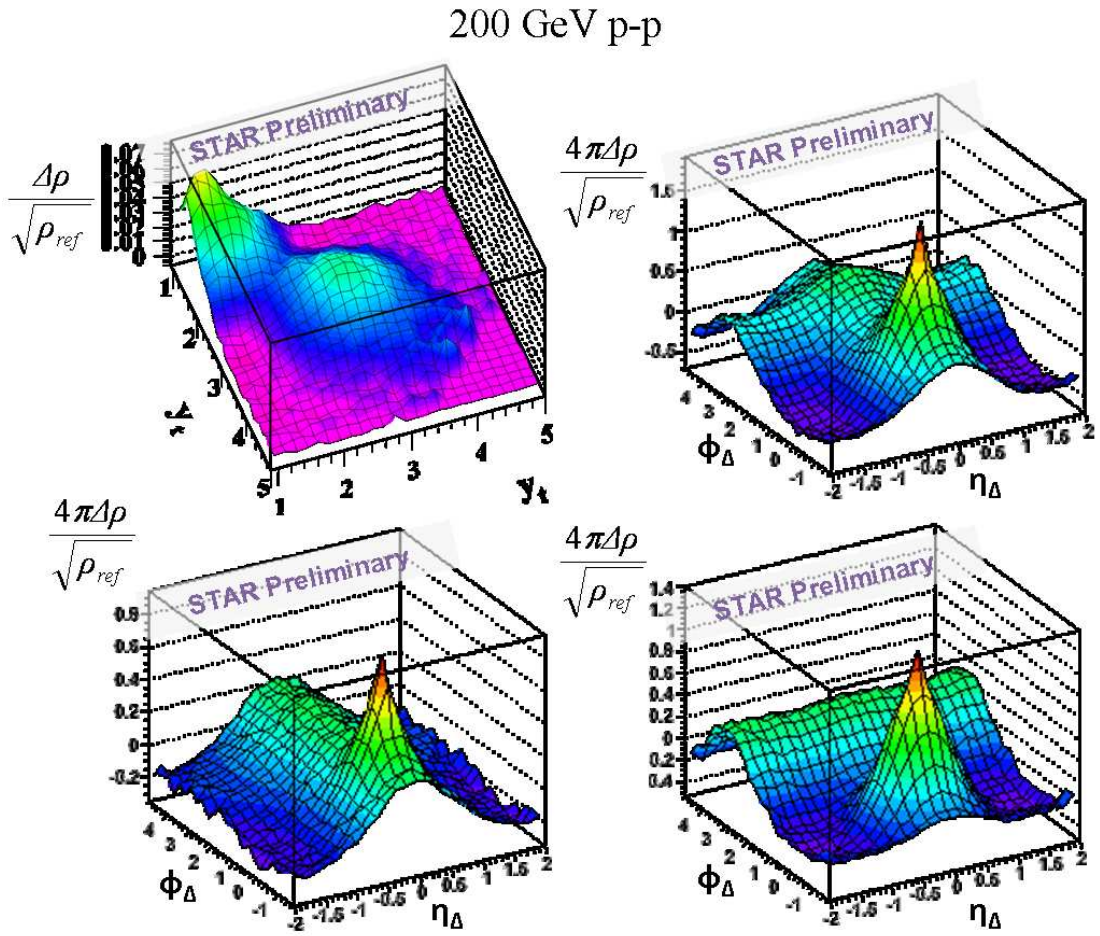

Figure 1: Two-particle (y_{t1},y_{t2}) (upper-left panel) and (η_Δ,ϕ_Δ) angular correlations (upper-right panel) for 200 GeV minimum-bias p-p collision data from STAR [5]. The angular correlations in the upper-right, lower-left and lower-right panels correspond to all pairs, pairs with $y_{t\Sigma} < 4$ and with $y_{t\Sigma} > 4$, respectively.

GeV/c. These correlated objects must have a minimum total energy of approximately 4 GeV, if unobserved neutrals are included, which is similar to the lower energy limit measured by UA1 for event-wise identified jets.

The UA1 observations were implemented theoretically as minimum-bias jets (i.e. no minimum p_t requirement imposed on the fragments, but $Q_0 > 2$ GeV per jet was required) in HIJING [8] using pQCD partonic cross sections and standard PDFs and FFs. HIJING predictions for 200 GeV p-p collisions with jets-on or off and no jet quenching are shown in Fig. 2. Reasonable agreement to about 20% with the STAR p-p correlation data for a $y_{t\Sigma} > 4$ pair selection cut in both the data and simulations is obtained. The UA1 energy cluster observations together with the HIJING minimum-bias jet pQCD predictions are two among several pieces of evidence which support a jet interpretation of the larger-y_t angular correlation structures, even for the relatively low fragment momenta included here.

In the present context "jet" refers to minimum-bias jets where no minimum p_t requirement is

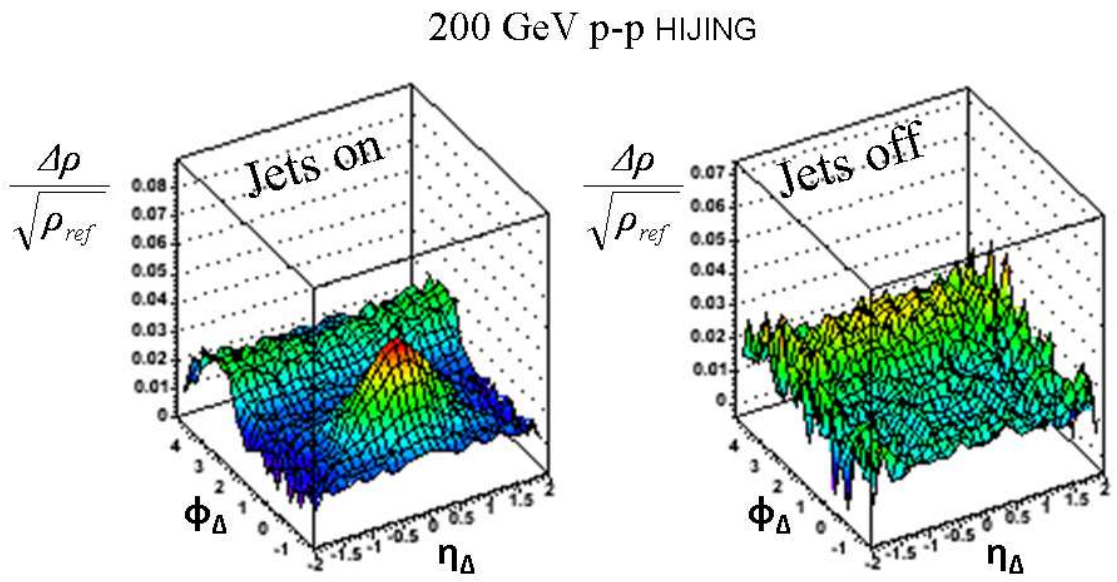

Figure 2: Default HIJING predictions for charged particle angular correlations for 200 GeV p-p collisions with pair $y_{t\Sigma} > 4$. Jets on (no quenching) and jets off options are shown in the left and right panels, respectively.

imposed on the final state particles. It is important to note that typical event-wise charged particle multiplicities associated with these jet structures are ∼2.5 [9]. Explicit jet reconstruction is therefore problematic and one must rely on inclusive correlation analysis [10] using all pairs (no trigger particle) to observe such objects.

4. Correlations for minimum-bias Au-Au collisions

Transverse rapidity correlations $\Delta\rho/\sqrt{\rho_{ref}}$ for 200 GeV minimum-bias p-p collisions and for three sample centrality bins from Au-Au minimum-bias collision data are shown in the respective four columns of panels in Fig. 3. Same-side (SS, $\phi_\Delta < \pi/2$), like-charge sign and unlike-charge sign pair correlations are shown in the first and second row of panels; away-side (AS, $\phi_\Delta > \pi/2$) LS and US pair corrleations are shown in the third and fourth rows. The p-p collision data (left-most panels in each row) are compared with the 84-93% peripheral, 28-38% mid-central and 0-5% central Au-Au collision data. The jet-like correlation peak at $y_t \sim 3$ is apparent in the AS (back-to-back correlations) plots from p-p to central Au-Au in both LS and US pairs. The SS, intra-jet two-particle correlations are dominated by US pairs and display a narrower distribution width along $y_{t\Delta} = y_{t1} - y_{t2}$ than that for the AS peak at $y_t \sim 3$. The former is likely due to gluon dominance for these mid-rapidity, low-energy jets and the very low, final state multiplicities in the minimum-bias jets (∼2.5). Baryon - meson decomposition of the SS correlation remains to be done. This additional analysis may provide further insight into the nature of the partonic origin of the SS peak. The larger width along $y_{t\Delta}$ for the AS peak relative to the SS is most naturally understood in terms of k_T broadening [11,12]. The persistence of the AS correlation peak at $y_t \sim 3$ all the way to most-central Au-Au collisions would not be expected for an opaque medium in which the recoil

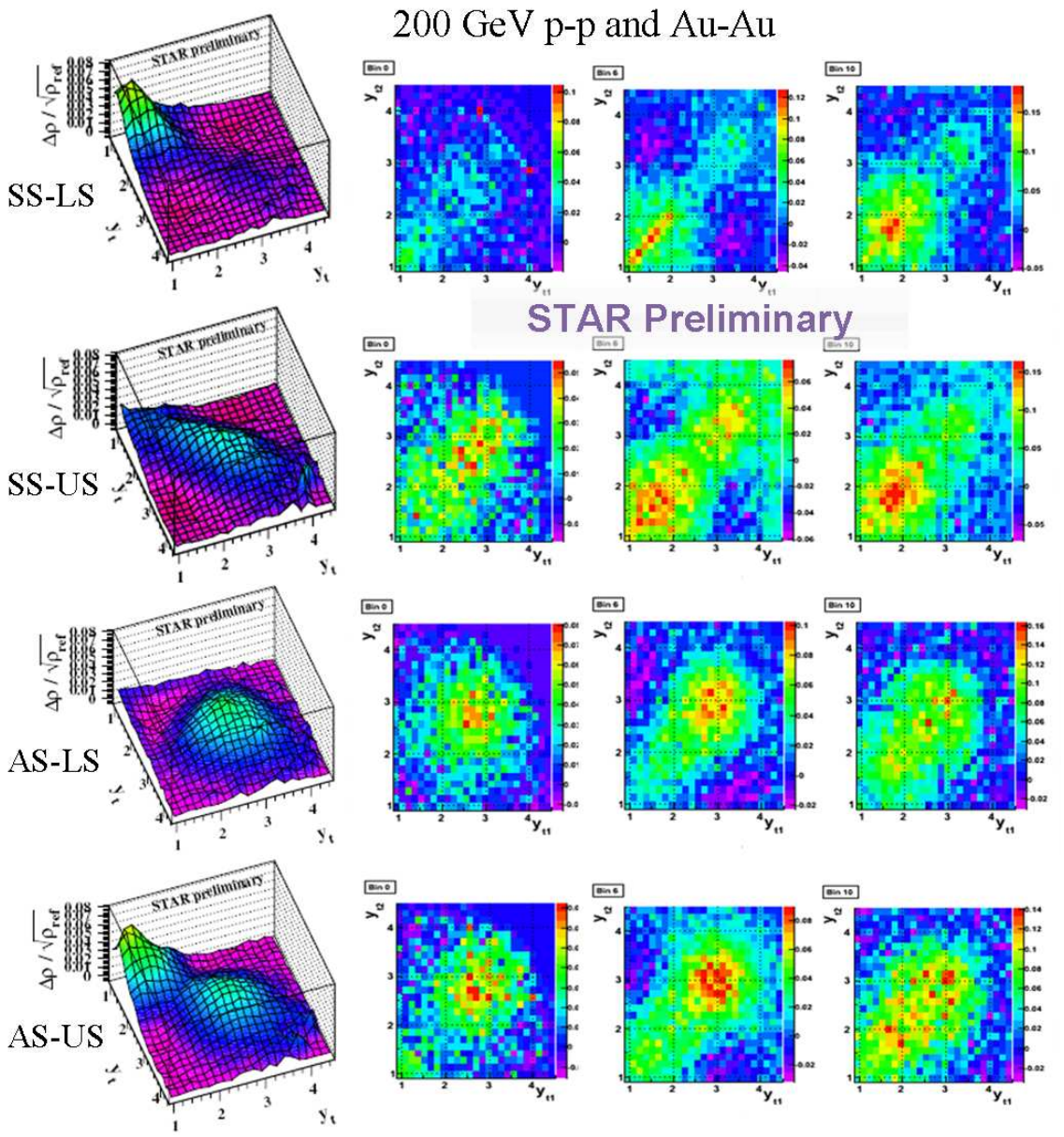

Figure 3: Two-particle correlations for 200 GeV p-p and Au-Au minimum-bias data on 2D transverse rapidity for SS-LS, SS-US, AS-LS and AS-US in the upper to lower rows, respectively. Perspective views in the left panels are for p-p data; the others are for selected Au-Au centralities of 84-93%, 28-38%, and 0-5% centrality from left-to-right, respectively.

momentum would be distributed to many final state particles, thus reducing the typical pair-wise momentum well below the 1 - 1.5 GeV/c range evident in Fig. 3. The increasing correlation amplitude with more central collisions for SS, US pairs at lower y_t may be related to the evolution of the η-elongated angular correlation peak structure known as the "ridge." However, a more detailed analysis is required to determine the p_t composition of the angular correlation structures [13].

The corresponding angular correlations for minimum-bias Au-Au and Cu-Cu collisions were presented at this workshop [12]. The measured distributions for the most peripheral (84-93%) Au-Au bin agree quantitatively with the p-p data and continue to have a very similar appearance to the p-p data until about mid-centrality at which point dramatic changes in the angular structures become evident with increasing centrality.

To quantify these centrality dependences the angular correlation data were fit with a model function based on the geometrical properties of the angular correlation structures observed in the p-p data using the LS and US and the lower and higher y_t cut selections. The higher y_t projections were accurately fit with a SS 2D Gaussian centered at (η_Δ,ϕ_Δ) = (0,0) plus an AS ridge, modelled either as a periodic Gaussian or as a dipole, $\cos(\phi_\Delta - \pi)$. The lower y_t data were accurately described with a 1D Gaussian ridge on η_Δ, centered at η_Δ = 0, plus a narrow 2D exponential representing quantum correlations and the e^+-e^- background. This geometrically motivated fitting model also accurately described the Au-Au correlation data provided a quadrupole term, $\cos(2\phi_\Delta)$, was added. The explicit fit model function for A-A collisions is [2],

$$\begin{aligned} F(\eta_\Delta,\phi_\Delta) &= A_3 + A_D\cos\phi_\Delta + A_Q\cos 2\phi_\Delta + A_0 e^{-\eta_\Delta^2/2\sigma_0^2} \\ &+ A_1 e^{-[\phi_\Delta^2/2\sigma_{\phi_\Delta}^2 + \eta_\Delta^2/2\sigma_{\eta_\Delta}^2]} + A_2 e^{-[\phi_\Delta^2/w_{\phi_\Delta}^2 + \eta_\Delta^2/w_{\eta_\Delta}^2]^{1/2}} . \end{aligned} \tag{4.1}$$

This fitting model was used to quantify and to compactly represent the centrality and energy dependences of the angular correlation data for the 62 and 200 GeV Au-Au and Cu-Cu minimum-bias data [12].

The amplitudes and the η_Δ and ϕ_Δ widths of the same-side 2D Gaussian components of the fit function for the 62 and 200 GeV Au-Au collision data are shown in Fig. 4 as a function of centrality parameter $\nu = 2\mathrm{N_{bin}}/\mathrm{N_{part}}$ (average number of binary collisions per participant nucleon) in comparison with the GLS trend. The amplitude increase above GLS, the large increase in the η_Δ width, and the azimuth narrowing summarize the essential geometrical properties of the p_t integrated same-side 2D peak or "ridge." The departure in the trend of these fit parameters away from GLS is referred to as a *transition*. It is also notable that the amplitude of the *away-side* ridge (dipole) is essentially proportional to the same-side 2D peak amplitude from peripheral to central collisions, as discussed in the next section. Global momentum conservation also results in an away-side ridge [14], however for quantity $\Delta\rho/\sqrt{\rho_{ref}}$ this contribution should remain approximately constant with centrality and cannot account for the large increase in the away-side ridge amplitude for more central collisions. Similar correlation structures were observed in the Cu-Cu data [12] although the increase above GLS is delayed until much more central collisions compared to that in Au-Au.

The HIJING predictions (jets on, no quenching) for Au-Au 200 GeV are indicated by the green triangle symbols and are seen to follow the GLS amplitude trend and to display constant widths

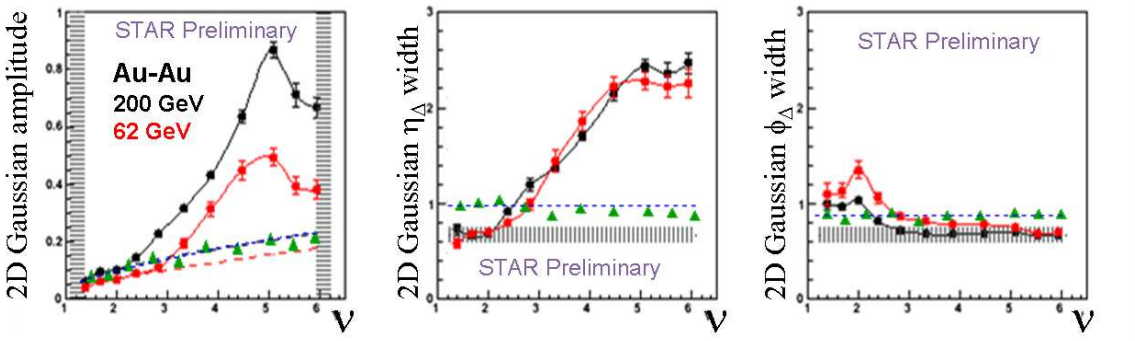

Figure 4: Fitted amplitudes and widths of the same-side 2D Gaussian model component for 200 GeV (black points) and 62 GeV (red points) Au-Au collision data as a function of centrality parameter $\nu = 2N_{bin}/N_{part}$. The dashed curves indicate the GLS estimate and the green triangle symbols are the 200 GeV HIJING predictions with jets-on and no-quenching.

with centrality as expected for N-N linear superposition. It is significant that the pQCD PDF - FF calculations encoded in HIJING [8] quantitatively predict the observed SS correlations in Au-Au collisions to near mid-centrality.

For the p-p correlation data, selection of pairs in (y_{t1},y_{t2}) space and projection onto angular correlations revealed much about the transverse momentum composition of the angular structures. Can a similar analysis procedure be used to quantify the p_t or y_t distributions of the particles which make-up the angular correlation structures discussed here, for example the same-side peak? To address this question the Au-Au (y_{t1},y_{t2}) subspace was sub-divided into four regions shown in the upper-left panel of Fig. 5 as suggested by the visible structures in the data there. The angular correlation quantity $\Delta\rho/\sqrt{\rho_{ref}}$ for the entire (y_{t1},y_{t2}) space was separated into weighted sums of normalized correlation quantities $\Delta\rho_i/\sqrt{\rho_{ref,i}}$ for each of the four regions i = 1, 2, 3 and 4 in Fig. 5, using the identity

$$\Delta\rho/\sqrt{\rho_{ref}} = \sum_{i=1}^{4} W_i \sqrt{\rho'_{ref}}\Delta\rho_i/\rho_{ref,i} \tag{4.2}$$

where weights $W_i = N_{ref,i}/N_{ref}$ are the ratios of the number of reference pairs in region i to the total. The four separate 200 GeV Au-Au data projections were fitted with the above model; the amplitude and widths of the SS 2D Gaussian are shown in Fig. 5. The 2D Gaussian amplitude and η width elongation are mainly determined by pairs in (y_{t1},y_{t2}) contained in the diagonal band centered at $y_{t\Sigma} = 4$ (blue band in on-line figure) and in the circle centered at $y_{t1} = y_{t2} = 3$ (red circle in on-line figure). Further subdivision of the (y_{t1},y_{t2}) space will enable a more quantitative determination of the p_t composition of the SS 2D peak [13].

Possible scaling variables for the SS 2D Gaussian amplitude and η_Δ width dependences on ion mass, collision energy, and centrality were studied. One candidate is the final-state transverse particle density estimated by $(3/2)(dN_{ch}/d\eta)(1/S)$ where S is a Glauber initial stage overlap area and factor 3/2 accounts for the unobserved neutral particles. Another candidate is the initial stage low-x parton overlap number estimated by $\rho_{profile}(A,b/2)\sigma_{NN}(\sqrt{s})$ where $\rho_{profile}(A,b/2)$ is the eikonal transverse density projection for nucleus A at a cylindrical radius equal to one-half the

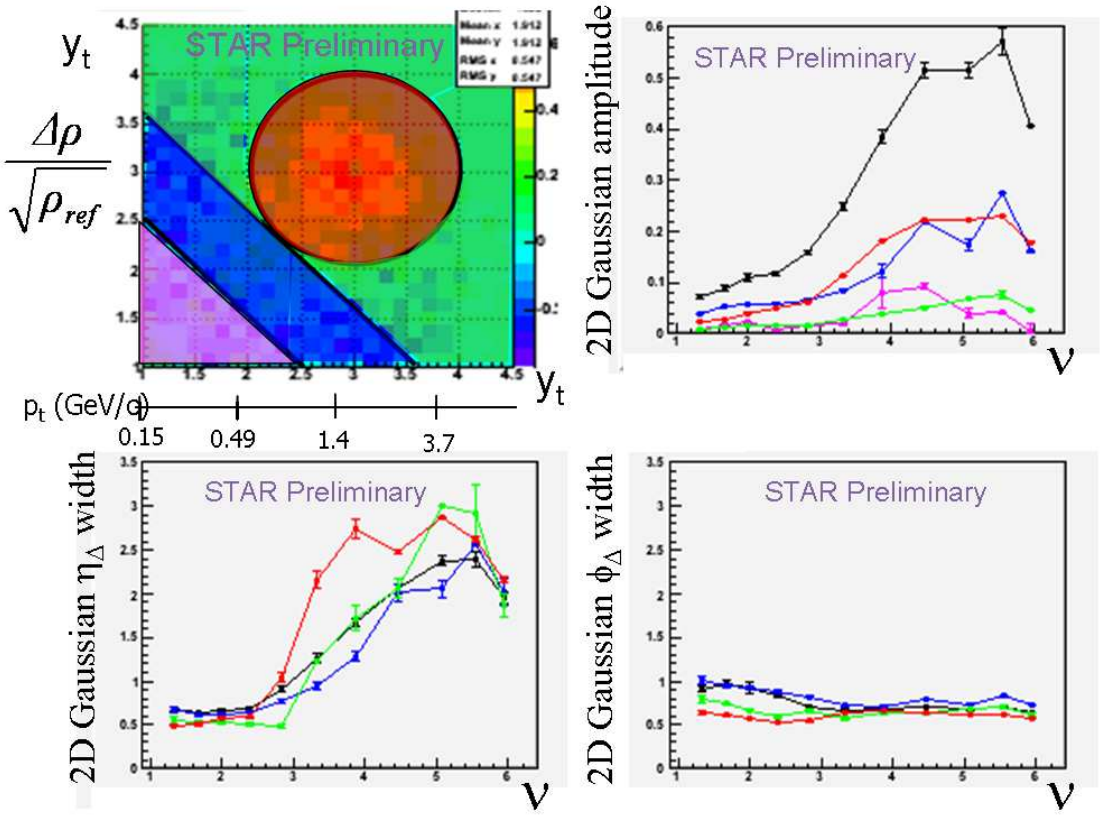

Figure 5: Transverse rapidity pair selections (upper-left panel) for 200 GeV Au-Au minimum-bias collision data and corresponding same-side 2D Gaussian fit parameters for the four regions indicated by colors magenta, blue, green and red, as a function of centrality parameter ν. (Note: this figure was corrected from the version shown during the workshop.)

impact parameter, $b/2$. The eikonal nuclear profile is a proxy for the low-x parton density. σ_{NN} is the nucleon-nucleon inelastic cross section, a proxy for the low-x partonic interaction area. Scaling based on the number of minimum-bias jets per collision is also being considered. Preliminary calculations indicate that initial stage overlap scaling provides a good description, however error estimates and further analysis remain to be done.

5. Discussion

STAR has accumulated considerable experimental information about the same-side peak and away-side ridge in 2D angular correlations. The same-side η_Δ-elongated correlation peak has been observed in 62 and 200 GeV Au-Au and Cu-Cu minimum-bias collision data for centralities beyond that where the transition away from GLS begins. The transition centralities are specific to each collision system and energy. The main features of the SS and AS correlation structures, summarized in parameters A_1, σ_{η_Δ}, σ_{ϕ_Δ} and A_D (dipole amplitude) defined in Sec. 4, include:

- The same-side 2D peak and the away-side ridge (dipole component) from p-p collisions to near mid-central A-A collisions are well described by perturbative QCD assuming GLS

(essentially binary collision scaling).

- Near mid-centrality, depending on the ion mass and beam energy, the centrality trend of the SS 2D peak and away-side ridge amplitudes begin to exceed the GLS estimates. The same-side η_Δ width increases significantly ("ridge" evolution), while the azimuth width of the same-side correlation peak decreases with centrality for the lower momentum particles < 1 GeV/c [13].

- The away-side ridge (dipole) amplitude closely follows that of the same-side peak, significantly exceeding both the GLS and global momentum conservation induced correlation estimates [2].

- Both the same-side 2D peak and the away-side ridge have direct correspondences with the correlation peaks at $y_t \sim 3$, or $p_t \sim$ 1-1.5 GeV/c, in the respective two-particle (y_{t1},y_{t2}) spaces. The η_Δ broadening in the centrality evolution of the same-side peak occurs for particles with transverse momenta between about 0.5 and 4 GeV/c [13].

- Charge-ordering is observed for the same-side correlation peak along η_Δ and ϕ_Δ [4], and also along $y_{t\Delta} = y_{t1} - y_{t2}$ by comparing the relative US and LS correlation amplitudes in Fig. 3.

- For central Au-Au collisions approximately 30% of the total charged particle production at mid-rapidity is associated with the same-side 2D peak [15].

Precise determination of the transverse momentum and particle identified composition of these correlation structures is underway. Pending the outcome of these studies the most natural explanation at this time for these specific correlation structures for p-p collisions up to the transition in A-A collision data is that these structures are caused by minimum-bias jets described by pQCD. Beyond the transition we may speculate about the origin(s) of these structures.

The AS dipole is generally attributed to some sort of p_t conservation. However, there is disagreement about the details. The away-side features, together with the corresponding AS (y_{t1},y_{t2}) correlation peak are significant in that they severely challenge theoretical models. The increased ϕ_Δ width of the AS ridge relative to that of the SS 2D Gaussian in a di-jet interpretation is indicative of k_T broadening effects which are qualitatively described by HIJING [16]. Radiative corrections and PDF may also affect the AS ridge width and amplitude. A broad, away-side $\cos(\phi_\Delta)$ ridge is also produced by "global" p_t conservation among the final-state particles. However, for quantity $\Delta\rho/\sqrt{\rho_{ref}}$ this contribution to the dipole amplitude is approximately constant with centrality and although it may account for a significant fraction of the dipole amplitude in p-p and peripheral A-A collision data, it is relatively negligible above the transition in A-A collisions where the dipole amplitude increases substantially as shown in Fig. 6.

Two-particle correlations between back-to-back di-jets in a strongly absorptive medium will be reduced or eliminated depending on the opacity of the medium and the jet total momentum. In the conventional model of RHIC collisions consisting of an opaque quark-gluon plasma "core" plus outer, weakly absorptive hadronic "corona" [17], unattenuated AS jet-like correlations should occur due to tangential emission from hard scattering processes in the outer corona. However, the centrality dependence of the resulting AS amplitude should follow a surface area scaling dependence and should therefore fall off relative to the SS amplitude due to the strong absorption

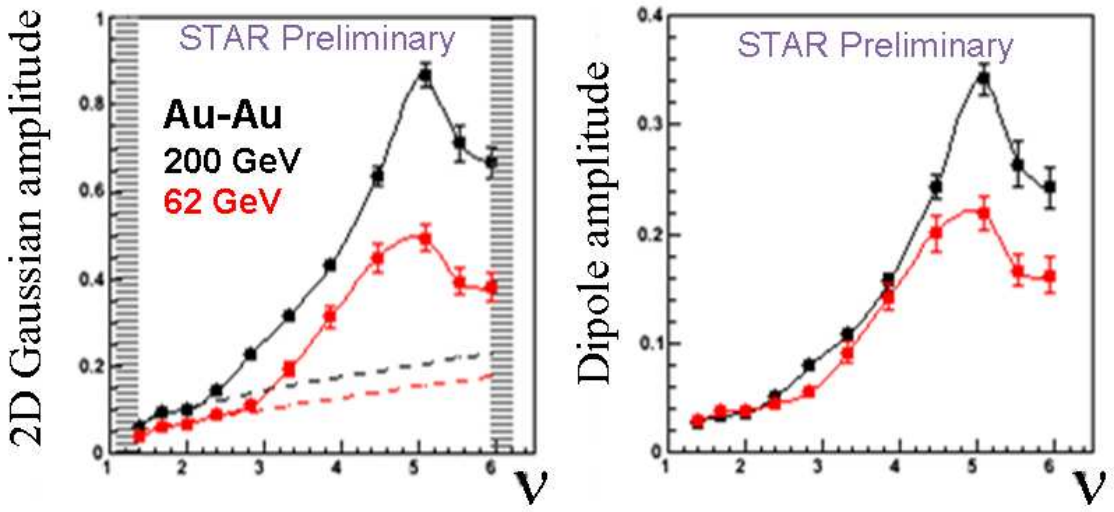

Figure 6: Comparison of the dipole and same-side 2D Gaussian amplitudes for 62 (red symbols) and 200 GeV (black symbols) Au-Au collisions as function of centrality parameter ν.

geometry of the system. Surface area scaling is in strong disagreement with the trends shown in Fig. 6. The general expectations for the AS structures for other theoretical models are discussed in the next section.

The agreement in both shape and magnitude of the SS and AS jet-like correlations with pQCD (HIJING) predictions from peripheral collisions to the transition implies that the collision system is essentially transparent to minimum-bias jets for these centralities. It may be surprising to recall that for this same centrality range and for charged particles with similar p_t the azimuth quadrupole [13] represented by v_2 is actually quite large. It is difficult to reconcile the seeming transparency of the system implied by the GLS scaling of jet-like correlations with the conventional pressure driven, hydrodynamic v_2 in terms of "elliptic flow." On the other hand, if the SS and AS correlations are not caused by pQCD jet processes but rather arise from hydrodynamic evolution of initial stage fluctuations for example, then it is difficult to reconcile this hydrodynamic scenario with the requirements of pQCD for collisions involving very few participant nucleons, which already accounts for most, if not all of the SS and AS structures. The same- and away-side correlation data discussed here and their trends on centrality severely challenge the hydrodynamic paradigm at RHIC. In contrast, the fact that the pQCD jet and fragmentation scenario discussed here does not account for the quadrupole correlation does not imply that the latter structure falsifies the existence of minimum-bias jets in RHIC collisions.

6. Constraints on theoretical models

Several theory groups have proposed models to explain the same- and away-side correlation structures. However, none has so far successfully addressed all of the observed properties summarized in the preceding section. There are generally two classes of models: (1) those in which an initial stage, spatially localized fluctuation creates long-range η_Δ correlations which are carried

outward by an assumed radial flow [18-22], and (2) those in which jet fragmentation and production is affected by an assumed strong rescattering and radial flow [23-27].

The initial stage fluctuation plus radial flow models will fail to describe the magnitude and centrality dependence of the AS ridge where the principle mechanism for producing the AS ridge in these models is overall p_t conservation. Furthermore, these models will not account for the magnitude and persistence of the two-particle AS (y_{t1},y_{t2}) correlation peak at $p_t \sim 1$ - 1.5 GeV/c because any recoil momentum will necessarily be distributed to many final-state particles by the assumed, strongly interacting medium. These models include viscous hydrodynamics with initial stage energy fluctuations [18,19], beam jets [20,21], and glasma flux tubes [22].

Jet driven models in which strong interaction with a viscous or non-viscous hydrodynamic medium is assumed will not likely be able to describe the rapid increase in amplitude above the GLS limit, the SS azimuth width narrowing, or the magnitude and persistence of the AS (y_{t1},y_{t2}) peak due to dissipation of the away-side jet into many final-state particles. These models include: jet-medium interaction models [23] assuming a viscous or non-viscous hydrodynamic medium, recombination between jet shower partons and the thermal partons of a medium producing localized hot spots in a longitudinally-expanding, radially-flowing medium [24], the jet driven momentum "kick" rescattering model [25], and models of plasma instability which induce longitudinal deflection of jet fragments [26,27].

7. Summary and conclusions

The intent of this workshop was to promote critical discussion of the RHIC data and several of the paradigms which have emerged for understanding the data. I have argued that the theoretical understanding of the centrality evolution of observables in ultra-relativistic A-A collisions must include pQCD predictions as a baseline before invoking additional or alternate physical mechanisms to explain the data. The present paper and others presented at this workshop [12,13,15] have shown that standard pQCD, PDFs and FFs provide a reasonable description of the minimum-bias jet-like aspects of two-particle correlation data from p-p collisions up to the transition in A-A collisions. The existence of large v_2 values at these same centralities and particle momenta where pQCD successfully accounts for the jet-like correlations is surprising if we assume that v_2 in peripheral to mid-central collisions is produced by strong partonic rescattering. Of course, jet fragmentation alone cannot account for the quadrupole correlation structure. For centralities above the transition both the same- and away-side jet-like correlation amplitudes increase significantly, as does the same-side η_Δ width. In addition, the two-particle, AS (y_{t1},y_{t2}) correlation peak persists at $p_t \sim 1 - 1.5$ GeV/c, which is the same p_t range where similar correlations are observed in p-p and peripheral A-A collision data.

Although each theoretical model may describe some of the same-side correlation features, none is able to describe all of the critical features of the correlation data reviewed here and in the other STAR correlation presentations at this workshop [12,13]. I therefore conclude that all of the present models of the formation of the SS correlation peak structure are falsified by the body of two-particle correlation data from STAR. The two-particle 2D correlation data presented at this workshop provide a crucial component of the experimental information needed to ultimately test and possibly falsify present and future RHIC paradigms. Moreover, these data provide the

most promising opportunity for the RHIC community to learn something new and lasting about the behaviour of strong-force systems in large-volume, dense environments and how QCD might be able to explain the resulting phenomena. Examples include the continuing and future study of modified fragmentation, gluon saturation, coherent parton scattering, and color radiation fields from extended collision systems.

This research was supported in part by the U. S. Department of Energy, Grant No. DE-FG02-94ER40845.

References

[1] J. Adams *et al*., (STAR Collaboration), Phys. Rev. C **73** (2006) 064907.

[2] M. Daugherity *et al*., (STAR Collaboration), J. Phys. G **35** (2008) 104090.

[3] K. H. Ackermann *et al*., (STAR Collaboration), Nucl. Instrum. Meth. A **499** (2003) 624.

[4] J. Adams *et al*., (STAR Collaboration), Phys. Lett. B **634** (2006) 347.

[5] R. J. Porter and T. A. Trainor, J. Phys: Conf. Ser. **27** (2005) 98.

[6] J. Whitmore, Phys. Rep. **27** (1976) 187.

[7] C. Albajar *et al*., (UA1 Collaboration), Nucl. Phys. B **309** (1988) 405.

[8] X.-N. Wang and M. Gyulassy, Phys. Rev. D **44** (1991) 3501.

[9] J. Adams *et al*., (STAR Collaboration), Phys. Rev. D **74** (2006) 032006.

[10] X.-N. Wang, Phys. Rev. D **46** (1992) R1900.

[11] E. Bruna, J. Phys.: Conf. Ser. **230** (2010) 012009.

[12] D. Prindle, in proceedings of the *Workshop on Critical Examination of RHIC Paradigms*, PoS(CERP2010)013.

[13] D. Kettler, in proceedings of the *Workshop on Critical Examination of RHIC Paradigms*, PoS(CERP2010)011.

[14] Z. Chajecki and M. Lisa, Phys. Rev. C **79** (2009) 034908.

[15] T. A. Trainor, Phys. Rev. C **80** (2009) 044901; and in proceedings of the *Workshop on Critical Examination of RHIC Paradigms*, PoS(CERP2010)003.

[16] M. S. Daugherity, Ph. D. Thesis, The University of Texas at Austin (2008), http://www.rhip.utexas.edu/publications/daugherity_dissertation.pdf

[17] K. Werner, Phys. Rev. Lett. **98** (2007) 152301.

[18] S. Gavin and M. Abdel-Aziz, Phys. Rev. Lett. **97** (2006) 162302.

[19] R. Andrade, F. Grassi, Y. Hama and W.-L. Qian, (2009) [arXiv:0912.0703].

[20] S. Voloshin, Nucl. Phys. A **749** (2005) 287c.

[21] E. Shuryak, Phys. Rev. C **76** (2007) 047901.

[22] K. Dusling *et al*., Nucl. Phys. A **836** (2010) 159.

[23] L. Pang, Q. Wang, X.-N. Wang and R. Xu, Phys. Rev. C **81** (2010) 031903(R).

[24] C. Chiu and R. Hwa, Phys. Rev. C **72** (2005) 034903.

[25] C.-Y. Wong, Phys. Rev. C **76** (2007) 054908.

[26] A. Majumder, B. Mueller and S. A. Bass, Phys. Rev. Lett. **99** (2007) 042301.

[27] A. Dumitru, Y. Nara, B. Schenke and M. Strickland, Phys. Rev. C **78** (2008) 024909.